CFD MODELING OF LH2 DISPERSION USING THE ADREA-HF CODE

Giannissi, S.G.[1,2], Venetsanos, A.G.[1], Bartzis[3], J.G., Markatos[2], N., Willoughby, D.B.[4] and Royle, M.[4]

[1] Environmental Research Laboratory, National Centre for Scientific Research Demokritos, 15310 Aghia Paraskevi, Attikis, Greece, email: sgiannissi@ipta.demokritos.gr, venets@ipta.demokritos.gr

[2] National Technical University of Athens, School of Chemical Engineering, Department of Process Analysis and Plant Design, Heroon Polytechniou 9, 15780 Zografou, Greece, email: n.markatos.@ntua.gr

[3] Department of Energy and Resources Management Engineering, University of West Macedonia, Kozani, Greece, email: bartzis@uowm.gr

[4] Health and Safety Laboratory, Buxton, Derbyshire, SK17 9JN, United Kingdom, email: Deborah.Willoughby@hsl.gov.uk, Mark.Royle@hsl.gov.uk

ABSTRACT

In the present work, the computational fluid dynamics (CFD) code ADREA-HF has been applied to simulate the very recent liquefied hydrogen spill experiments performed by the Health Safety Laboratory (HSL). The experiment consists of four LH2 release trials over concrete at a fixed rate of 60 lt/min, but with different release direction, height and duration. In the modeling, the hydrogen source was treated as a two phase jet, enabling simultaneous modeling of pool formation, spreading as well as hydrogen vapor dispersion. Turbulence was modeled with the standard k-ε model modified for buoyancy effects. The effect of solidification of the atmospheric humidity was taken into account. The predicted concentration at the experimental sensors' locations was compared with the observed one. The results from the comparison of the predicted concentration with and without solidification of the atmospheric humidity indicate that the released heat from the solidification affects significantly the buoyant behavior of the hydrogen vapor. Therefore the simulation with solidification of the atmospheric humidity is in better agreement with the experiment.

1.0 INTRODUCTION

Hydrogen is a well promising alternative fuel, due to its big energy carrier and friendly to environment use. However, it has some drawbacks that limit its widespread use with the present technology. These drawbacks are related to its production, handling, storage, and transportation. Hydrogen in ambient conditions is gas with low density. So, hydrogen storage and transportation is usually accompanied with its liquefaction at low temperature and high pressure. If during an accident the liquefied hydrogen (LH2) is released, it produces a cold, dense mixture at the beginning that remains at the release site for longer duration, increasing the danger factor. After a while the mixture is being heated by the surroundings (the ambient air, the ground, etc.) and becomes lighter than the air so it is more buoyant and can be diluted in air more easily, avoiding the creation of a hazardous, combustible mixture.

In this framework a lot of experimental and computational efforts have been orientated towards the study of the conditions that influence the dispersion of hydrogen under cryogenic release conditions, and they try to determine the factors that could mitigate the consequences of such an accident. Recent LH2 spill experiments have been conducted by the Health Safety Laboratory (HSL) [1]. They consist of 4 tests with the same release rate, but with different source location. Temperature data at several distances downwind the release point and soil temperatures are available.
In this paper test 5 of the HSL experiments has been simulated using the ADREA-HF code. ADREA-HF is a computational fluid dynamics (CFD) code [2], which solves the three dimensional mass, energy, and momentum conservation equations of a mixture with the finite volume method. Earlier

work related to CFD modeling of LH2 dispersion using the ADREA-HF code is the simulation of the BAM experiments [3] and the NASA experiments [4].

The main interest of the present work is to study how atmospheric humidity influences the hydrogen vapor dispersion. When moisture is present in the atmosphere affects the hydrogen cold behavior, because the condensation and solidification of the water vapor liberates heat. Consequently, the buoyancy of the cloud is enhanced and the gravitation-induced spreading is limited. The computational results with and without atmospheric humidity are compared with each other and with the experimental measurements.

2.0 THE HSL EXPERIMENTS

The HSL experiments were conducted by the Health and Safety Laboratory in 2010. These experiments are related to hydrogen release and dispersion in open environment. Four spill tests have been performed. During these tests liquefied hydrogen (LH2) was released through a nozzle with release rate 60 lt/min and different release direction, height and duration in each spill test. The release point was above a concrete pad of 32 m diameter. Figure 1 is a site plan showing the layout of the tests. For all test cases, relative humidity (RH), ambient temperature, wind speed and wind direction measurements at 2.5 m height are available.

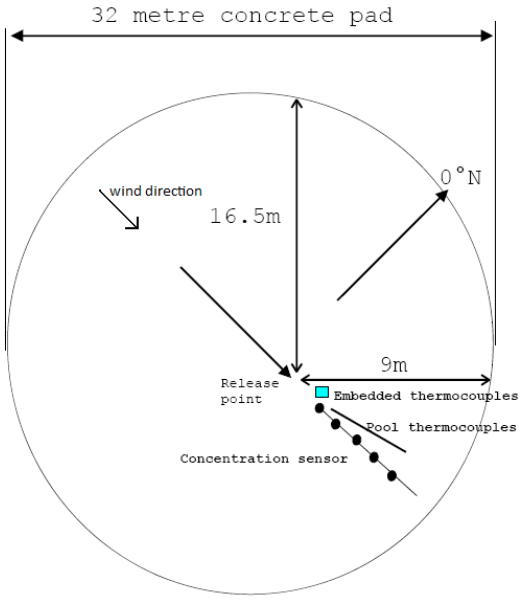

Figure 1.HSL test layout (not drawn to scale).

For monitoring the H2 concentration 30 oxygen depletion sensors were deployed. The sensors were placed in line with the wind direction at 1.5, 3, 4.5, 6, and 7.5 m downwind the release point and at 0.25, 0.75, 1.25, 1.75, 2.25, and 2.7 m height. However, the oxygen sensors were severely affected by the condensed water within the hydrogen cloud and the extreme low temperature. Therefore, another approach was used to obtain the H2 concentration. Along with the oxygen sensors, type E thermocouples were deployed at the exact same location to measure the cloud temperature. An initial H2 concentration level was derived by the temperature data assuming adiabatic mixing [5] and then it was corrected by taking into account the relative humidity in the calculation. There are also available soil temperature measurements in 10, 20 and 30 mm depth inside the concrete.

They were positioned 1.5 m from the release point and 0.2 m offset from the center line of the release. Finally, ground level pool thermocouples were placed in line with the release with the first thermocouple 500 mm from the release point. They were mounted into a frame and spaced 100 mm apart in a horizontal line.

Table 1 shows the release and weather conditions for test 5, that is simulated in the present work. The absolute storage pressure was measured immediately upstream of the release valve with the tanker valve open and the release valve closed. The absolute release pressure was measured immediately upstream of the release valve with the release valve open.

Table 1. Release and weather conditions for test 5

source diameter (mm)	26.6
source height (mm)	3.36
source direction	horizontal
release rate (kg/sec)	0.07
release duration (sec)	248
absolute storage pressure (bar)	2
absolute release pressure (bar)	1.2
wind speed (m/s) at 2.5m height	2.675
wind direction (deg) at 2.5m height	291.02
average ambient temperature (K) at 2.5m height	283.56
relative humidity (%)	68

3.0 METHODOLOGY

3.1 Governing equations

It is assumed a multi-component mixture in thermodynamic equilibrium. The mean flow is described by the conservation equations for the mixture mass, momentum, energy and the chemical species. This set of equations is respectively

$$\frac{\partial \rho}{\partial t} + \frac{\partial \rho u_i}{\partial x_i} = 0 \tag{1}$$

$$\frac{\partial \rho u_i}{\partial t} + \frac{\partial \rho u_j u_i}{\partial x_j} = -\frac{\partial P}{\partial x_i} + \rho g_i + \frac{\partial}{\partial x_j}\left((\mu + \mu_t)\left(\frac{\partial u_i}{\partial x_j} + \frac{\partial u_j}{\partial x_i} \right) \right) \tag{2}$$

$$\frac{\partial \rho H}{\partial t} + \frac{\partial \rho u_j H}{\partial x_j} = \frac{\partial}{\partial x_j}\left(\frac{\mu_t}{Pr_t} \frac{\partial H}{\partial x_j} \right) + \frac{dP}{dt} + \frac{\partial}{\partial x_j}\left(\lambda \frac{\partial T}{\partial x_j} + \sum_i dH_i \frac{\partial q_i}{\partial x_j} \right) \tag{3}$$

$$\frac{\partial \rho q_i}{\partial t} + \frac{\partial \rho u_j q_i}{\partial x_j} = \frac{\partial}{\partial x_j}\left(\left(\rho d + \frac{\mu_t}{Sc_t} \right) \frac{\partial q_i}{\partial x_j} \right) \tag{4}$$

The mixture density is calculated based on the density of each component in each phase with its mass fraction in the mixture:

$$\frac{1}{\rho} = \sum \frac{q_{iv}}{\rho_{iv}} + \sum \frac{q_{inv}}{\rho_{inv}} \tag{5}$$

For the sum of all components' mass fraction and for the mass fraction of each component in each phase the following relationships are applied:

$$\sum q_i = 1 \tag{6}$$

$$q_{iv} + q_{inv} = q_i \tag{7}$$

In the above equations ρ is the mixture density (kg/m^3), u is the velocity vector (m/s), P is the pressure (Pa), g is the gravity vector (m/s^2), μ and μ_t are the laminar and turbulent viscosity respectively (kg/m/s), Pr_t is the dimensionless turbulent Prandtl number, d is the molecular diffusivity of hydrogen to air (m^2/s), λ is the thermal conductivity (W/K/m), Sc_t is the dimensionless turbulent Schmidt number, H is the enthalpy, and q is the mass fraction. Prandtl number and Schmidt number are set equal to 0.72. The subscripts i, j denotes the component i and the Cartesian j coordinate respectively, and v, nv stands for the vapor and non vapor phase (liquid and solid).

For the phase distribution in the mixture the following assumption is applied: The liquid phase appears, when the temperature is equal or lower than the mixture saturation (dew) temperature.

$$T \le T_s \tag{8}$$

where s subscript – saturation level

The mixture dew temperature is obtained iteratively from the following relationship, which is derived from Raoult's law for ideal mixtures [6]:

$$P = \frac{\sum \frac{q_j}{M_j}}{\sum \frac{q_j}{M_j P_{Sj}(T)}} \tag{9}$$

where M_j - the molecular weight of component j; P_{sj} the saturation pressure for component j.

The vapor mass fractions are calculated iteratively according to Raoult's law for ideal multi-component mixtures and by requiring the sum of the molar fractions in the liquid phase to be equal to one. The liquid mass fractions can be obtained from the vapor mass fractions and the total mass fractions of each component.

In addition, the solid phase of component-i appears when the mixture temperature drops below the freezing point of component-i.

Turbulence was modeled using the k-ε model with buoyancy source term [7].

3.2 The source term

Hydrogen is released under cryogenic conditions. As soon as it is released, flash vaporization is occurred due to pressure reduction. More specifically, hydrogen in the tanker is a saturated liquid at 2 bars pressure. After the valve is open the pressure drops at 1.2 bars and part of hydrogen is instantaneously vaporized. In the simulation the source was modeled as a two phase jet, so at source boundary a mixture of liquid and vapor hydrogen is assumed. The exact amount of hydrogen that has

been vaporized is calculated assuming isenthalpic expansion. The following equation is used to predict the vapor mass fraction of hydrogen that has been vaporized:

$$q = \left(H_{1\ell} - H_{2\ell}\right) / \left(H_{2v} - H_{2\ell}\right) \tag{10}$$

Subscripts 1, 2, are for the pressure conditions before and after the exit respectively. The mixture density can be calculated by the H_2 vapor mass fraction at the source using the relationship:

$$\frac{1}{\rho_{mix}} = \frac{q_v}{\rho_v} + \frac{q_\ell}{\rho_\ell}$$
$$q_\ell = 1 - q_v \tag{11}$$

The vapor and liquid densities were at the release pressure and temperature. The mass release rate can be calculated by multiplying the experimental volumetric release rate with the mixture density, and next the mixture velocity at the release point can be obtained knowing the release area.

3.3 Ground heat transfer

In previous work [3] it is shown that heat transfer from the ground plays an important role in hydrogen dispersion. Heat makes the vapor cloud more buoyant and as a consequence it rises more. Therefore, ground heat transfer was modeled by solving a transient one dimensional temperature equation in the underground.

$$\rho c_P \frac{\partial T}{\partial t} = \lambda \frac{\partial^2 T}{\partial z^2} \tag{12}$$

where c_P -heat capacity, J/kg·K.

To solve the temperature equation the physical properties of the ground are necessary. The release in HSL experiments was above concrete, but the exact type of concrete or its properties are not known. A Portland limestone was assumed with density $\rho = 2371 kg/m^3$, heat capacity $c_p = 880 J/kg \cdot K$ and thermal conductivity $\lambda = 1.13 W/m \cdot K$, but the need for further information or investigation is necessary.

3.4 Humidity effect

During the HSL experiments high levels of humidity were observed (~68%). Due to that fact, an additional conservation equation for the water vapor was solved, in order to determine the humidity effect on hydrogen dispersion.

As mentioned in the introduction the ambient moisture, when it is in high levels, contributes to the buoyant behavior of the hydrogen cloud, because of the heat liberation due to the condensation and solidification of the water vapor in such low mixture temperatures. The mass fraction of the water was calculated by the relative humidity based on the relationships below and found equal to 0.00529:

$$RH = 100 \cdot \frac{p_{H_2O}}{p^*_{H_2O}} \tag{13}$$

$$q_{H_2O} = M_{H_2O} \cdot p_{H_2O} \Big/ \left(M_{dryair} \cdot \left(P - p_{H_2O}\right) + M_{H_2O} \cdot p_{H_2O}\right) \tag{14}$$

where RH-relative humidity; p_{H_2O} - the partial pressure of water vapor in the gas mixture; $p^*_{H_2O}$ - the saturation vapor pressure of water at mixture temperature; P - the atmospheric pressure.

Figure 2 shows the non vapor mass fraction of the water and the mixture temperature during the experiment at the closest to the source sensor (1.5, 0, 0.25) for test 5. The mixture temperature is from the experimental data and the condensed and solidified water vapor mass fraction is calculated with the help of the package of component physical properties that is available in ADREA-HF code. It is observed that when the mixture temperature drops, as soon as the release starts, the water vapor begins to condense and at temperature levels below the freezing point is solidified. At some times, the whole mass of water vapor is condensed or solidified. That fact along with the high latent heat of water condensation and solidification per unit mass leads to the need to examine whether humidity effect is significant.

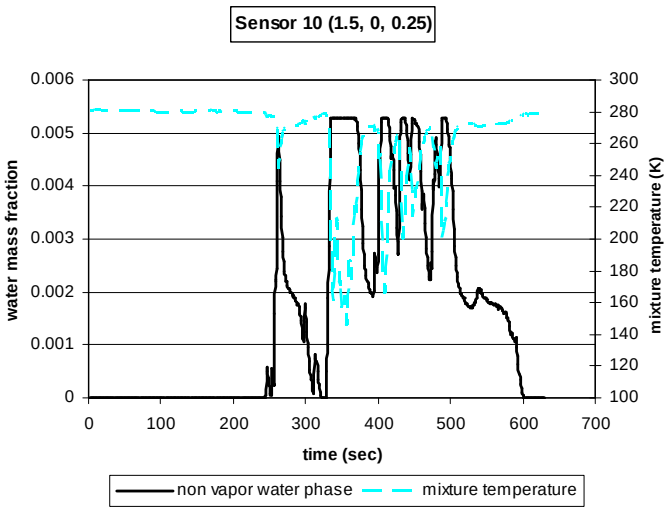

Figure 2. The mixture temperature according to the HSL test 5 experiment and the calculated condensed or solidified water mass fraction at sensor 10 versus time.

4.0 SIMULATION SETUP

The simulation domain and the grid at level z=0 is depicted in Figure 3. The zoomed area inside the rectangular contains the source (yellow arrow) and the sensors' location (orange spheres). The arrow's direction corresponds to the release direction, which is horizontal in test 5. The domain dimension are $80 \times 70 \times 20$ m in the x, y, z direction respectively. The origin corner is at x = -20, y = -35 and z = 0. The grid consists of 100 188 cells ($66 \times 66 \times 23$). Close to the source the grid is denser with minimum cell size 0.1m in x and y direction and 0.2 in z direction.

According to HSL experiments, LH2 with release rate 60lt/min was spilled 3.36 mm above concrete in horizontal direction. The release data used in the present work were 17.4468 kg LH2 total mass spilled with horizontal velocity 6.0209 m/s, and almost 71.34 vol% LH2 was flashed vaporized. When atmospheric humidity was modeled, the initial condition for the water vapor content in ambient moist air was 0.529 wt.%.

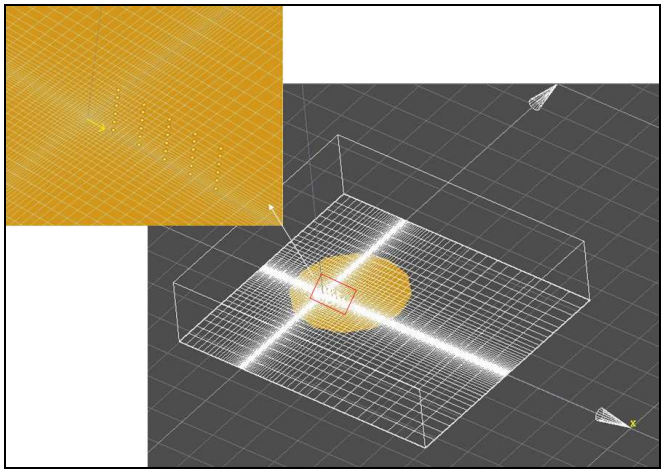

Figure 3. The simulation domain ($80 \times 70 \times 20$ m) and the grid at level z=0. The zoomed area is the area close to the release point and depicts the source (yellow area) and the sensors (orange spheres).

The simulation procedure consists of three parts. First, one dimensional steady problem is solved, in order to obtain the wind profile using the experimental data. Next, three dimensional steady problem is solved using as initial conditions the values of the first part, to obtain the initial wind field within the domain. Finally, the three dimensional transient problem with LH2 release is solved, with initial conditions and wind profile the values from the second part.

5.0 RESULTS AND DISCUSSION

Figure 4 compares the predicted hydrogen concentration (by volume) when ambient humidity was neglected, with the predicted hydrogen concentration with humidity effect and the measured one at different distances downwind the release point. The release starts at 244 sec.

The case without the humidity effect tends to overpredict the hydrogen concentration at the sensors far from the spill point, revealing that the cloud travels more downwind than the experiment. When ambient humidity is taken into account in the simulation, the prediction is improved to a great extent compared with the one without the humidity effect. The predicted concentration is decreased, and is closer to the experiment.

Figure 5 depicts the concentration histories at 7.5 m downwind the release point and at different heights from the ground. In the case without humidity effect, the cloud stays at low heights, in contrast to the experiment, while the case with humidity effect predicts higher concentration at bigger heights and approximates very well the experiment. The above behaviour indicates that the presence of moisture in the atmosphere makes the cloud more buoyant, because of the heat liberation by the water condensation and solidification.

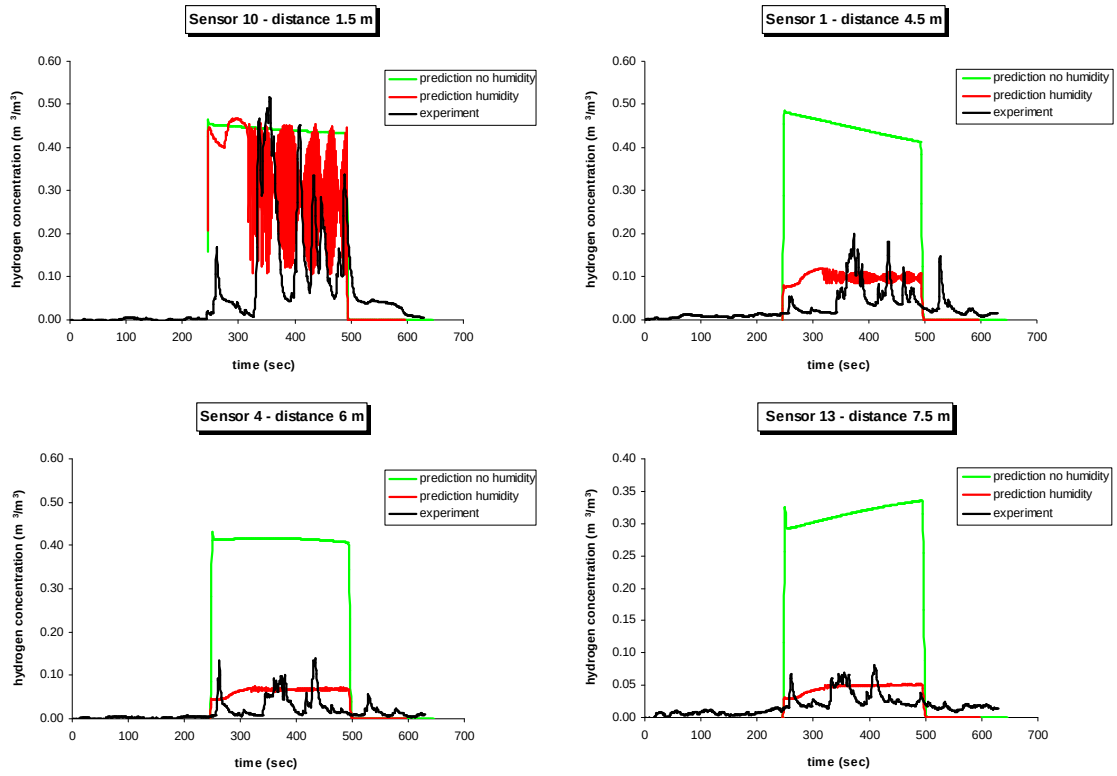

Figure 4. The hydrogen concentration histories for both cases (without and with humidity effect) versus the measured ones. The sensors are at 0.25 m height and distances 1.5, 4.5, 6, 7.5 m downwind the release point.

Figure 6 shows the predicted contours of hydrogen concentration on the plane y=0 in the release line 20 sec after the start of the release for both cases (time=264s). The black dots represent the location of some sensors. As shown in the figure the LFL (4 vol%) of the cloud in the case without humidity is extended downwind at 25m and reaches almost 2 m height. In the case with humidity the LFL of the cloud is extended downwind at 15 m and rises up to 3m. In general, the flammable cloud in the case with humidity effect seems to be restricted in the area near the source, and therefore the danger is diminished.

Figure 7 displays the hydrogen contours for both cases on the plane y=0 at 364 sec. The buoyant behavior of the cloud, especially in the case with humidity effect, is now less obvious compared to the 264 sec time. This happens due to the reduction of heat transfer from the ground, which is another factor that influences the buoyancy-driven behavior of the cloud. At the start of the release the ground has higher temperature, but as the release continues the ground becomes colder. Less heat transfer from the ground contribute to the reduction of the buoyancy force.

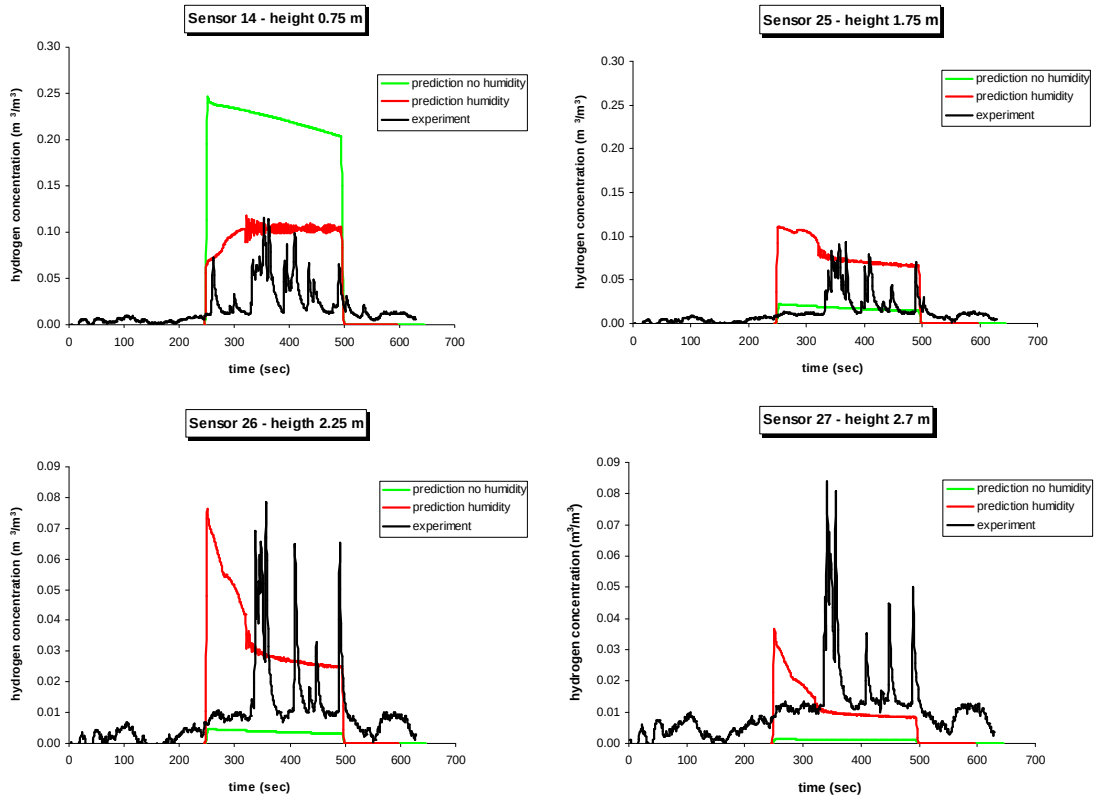

Figure 5. The hydrogen concentration histories for both cases (without and with humidity) versus the measured ones. The sensors are at 7.5 m downwind the release point and at different heights from the ground.

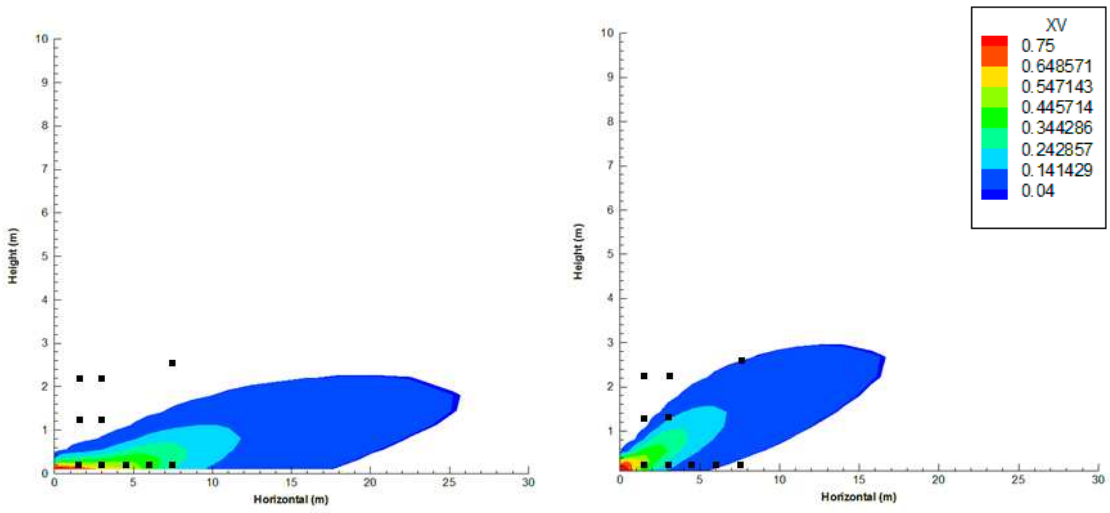

Figure 6. Predicted contours of hydrogen concentration (by vol.) on plane y=0 in the release line at 264 s. (left: case without humidity effect, right: case with humidity effect).

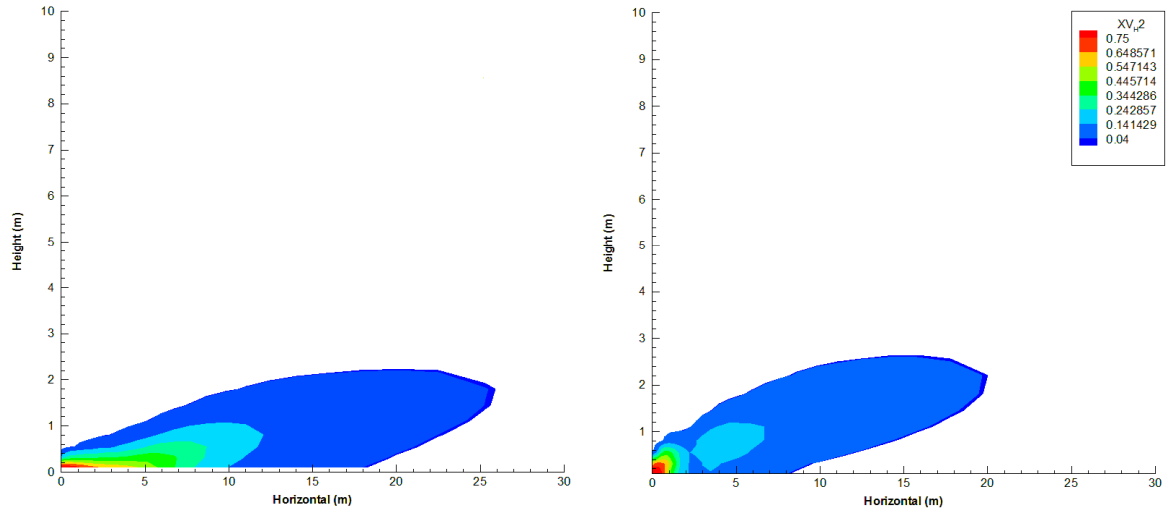

Figure 7. Predicted contours of hydrogen concentration (by vol.) on plane y=0 in the release line at 364 s. (left: case without humidity effect, right: case with humidity effect).

To evaluate further the performance of the simulation, statistical measures were applied. The parameters that are usually used for dense gas dispersion model [8] are the fractional bias (FB), the normalised mean square error (NMSE), the mean relative bias (MRB), the mean relative square error (MRSE), the geometric mean (MG), and the geometric mean variance (VG). At present work MG and ln(VG) are decided more appropriate to use:

$$\mathrm{MG} = \exp\overline{\left(\ln \mathrm{C_p} - \ln \mathrm{C_o}\right)} \quad , \quad \ln\left(\mathrm{VG}\right) = \overline{\left(\ln \mathrm{C_p} - \ln \mathrm{C_o}\right)^2} \tag{15}$$

where $\mathrm{C_p}$ is the time average predicted concentration, $\mathrm{C_o}$ is the time average observed concentration, and the overbar denotes the mean for all 30 sensors.

Table 2 displays the calculated values of these parameters for both cases (without and with humidity effect) and the ideal values. The time average value corresponds to the mean value of concentrations that are over 10% of the maximum concentration in each sensor.

Table 2. The statistical performance measures for the test 5-HSL experiment for both cases (without and with ambient humidity effect)

	MG	ln(VG)
ideal value	1	0
without humidity	0.22	12.18
with humidity	0.84	4.7

The statistical evaluation suggests that the case with humidity effect is closer to the experimental observations. The value of MG smaller than 1 in both cases indicates that overall the model underestimates the concentration compared to the experimental values.

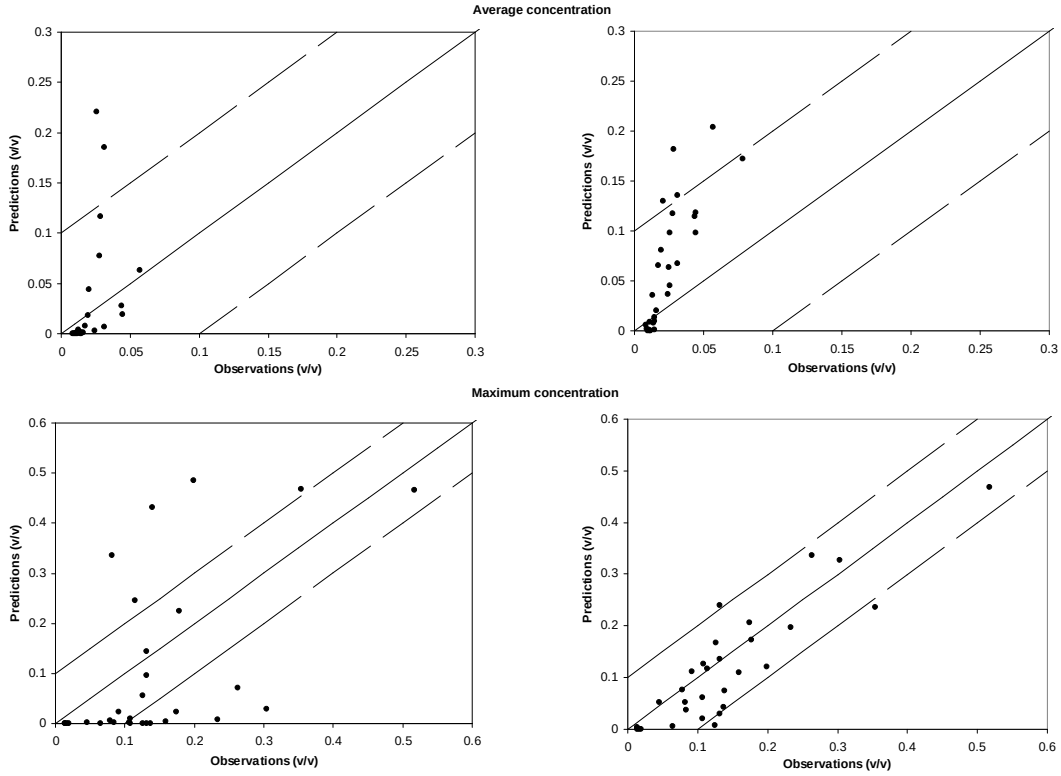

Figure 8. Scatter plot for predicted versus observed concentration histories for both cases (left: without humidity, right: with humidity, top: average concentration, bottom: maximum concentration).

In Figure 8, a scatter plot for both cases and for all the experimental sensors is depicted. The graph shows the average predicted and the maximum predicted concentration versus the observed one. Both average and maximum predicted concentration for the case without humidity effect are underestimated for most of the sensors, since most of the points are below the diagonal line. In the case with humidity effect and as far as the predicted maximum concentration is concerned almost all sensors are in good agreement with the experiment within a factor of 2. The average predicted concentration for most of the sensors is within a factor of 2 and generally is overpredicted, because the majority of the statistical points are left of the diagonal line.

6.0 CONCLUSIONS

In this paper, the ADREA-HF code was applied to simulate the test 5-HSL experiment related to LH2 release. In particular, the ambient humidity effect in the hydrogen cloud dispersion was investigated. The predicted concentration for both cases (without and with humidity effect) was compared with the measured concentration. It is concluded by the concentration histories that the prediction in the case with humidity effect is in better agreement with the experiment.

According to the prediction, when moisture is present in the atmosphere, the cloud becomes more buoyant. This is happening because of the heat liberation by the water vapor condensation and solidification. It seems that initially the amount of the released heat is enough to force the cloud to lose its dense behavior.

As a consequence of the above remark, in the case with humidity effect the cloud rises higher and the downwind distance that the LFL of the cloud extends is reduced almost 40% of the distance that it extends in the case without humidity at the early stage of the release. That means that when the ambient air is moist, the flammable and hazardous cloud is restricted to smaller area near the release, and it does not remain close to the ground.

Quantitative validation of the dispersion model was performed using statistical performance measures. The conclusions that were drawn from the quantitative assessment are consistent with the ones derived from the qualitative assessment. According to the statistical performance analysis the prediction with humidity effect gives better results, closer to the experimental behavior. Finally, the model overall underestimates the hydrogen concentration for both cases.

All the above suggests that humidity in high levels in the atmosphere can influence to a great extent the hydrogen dispersion and the formed, hazardous cloud, so it should be taken into account in experiments and simulations related to cold gas dispersions.

REFERENCES

1. Willoughby, D.B., Royle, M., Experimental Releases of Liquid Hydrogen, 4th *International Conference on Hydrogen Safety*, San Francisco, California-USA, ICHS , Paper 1A3, 2011.
2. Venetsanos, A.G., Papanikolaou, Bartzis, J.G., The ADREA-HF CFD Code for Consequence Assessment of Hydrogen Applications, *Hydrogen Energy Journal*, **35**, 2010, pp. 3908-3918.
3. Statharas, J.C., Venetsanos, A.G., Bartzis, J.G., Würtz, J., Schmidtchen, U., Analysis of Data from Spilling Experiments Preformed with Liquid Hydrogen, *Hazardous Material Journal,* **A77,** 2000, pp. 57-75.
4. Venetsanos, A.G., Bartzis, J.G., CFD Modeling of Large-Scale LH2 spills in open environment, *Hydrogen Energy Journal,* **32,** 2007, pp. 2171-2177.
5. Witcofski, R.D., Chirivella, J.E., Experimental and Analytical Analyses of the Mechanisms Governing the Dispersion of Flammable Clouds Performed by Liquid Hydrogen Spills, *Hydrogen Energy Journal*, **9**, No. 5, 1984, pp. 425-435.
6. Tassios, D.P., Applied Chemical Engineering Thermodynamics, 1993, Springer-Verlag, New York.
7. Launder, B.E., Spalding, D.B., The Numerical Computation of Turbulent Flow, *Computer methods in applies mechanics and engineering Journal,* **3,** No. 2, 1974, pp. 269-289.
8. Duijm, N.J., Ott S., Nielsen, M., An Evaluation of Validation Procedures and Test Parameters for Dense Gas Dispersion Models, *Loss Prevention Process Ind. Journal*, **9**, No. 5, 1996, pp. 323-338.